


Article

Long Term Skeletal, Alveolar, and Dental Expansion Effects of the Midfacial Skeletal Expander

Catherine Ding ^{1,†}, Ney Paredes ^{1,*,†} , Ben Wu ² and Won Moon ^{2,3,*}

¹ Section of Orthodontics, Division of Growth and Development, School of Dentistry, Center for Health Science, University of California, Los Angeles, Room 63-082 CHS, 10833 Le Conte Ave, P.O. Box 951668, Los Angeles, CA 90095-1668, USA; catherineding418@gmail.com

² The Forsyth Institute, Affiliate of HSDM, 245 First Street, Cambridge, MA 02142, USA; bwu@forsyth.org

³ Department of Orthodontics, Institute of Oral Health Science, Ajou University School of Medicine, Suwon 16499, Republic of Korea

* Correspondence: neyalbertoparedes@gmail.com (N.P.); themoonprinciples@gmail.com (W.M.)

† Co-First author.

Abstract: Background: The Midfacial Skeletal Expander (MSE) produces a greater skeletal effect than its dentoalveolar side effects. The aim of this study was to quantify the stability of the different components of MSE expansion post-orthodontic treatment. Methods: Fourteen subjects (mean age of 20.4 ± 3.5 years) were treated with the MSE. The pre-expansion (T0), post-expansion (T1), and post-treatment (T2) CBCT records were superimposed and compared. The rotational fulcrum of the zygomaticomaxillary complex was identified, and angular measurements were generated to assess changes in the zygomaticomaxillary complex (skeletal expansion), dentoalveolar bone (alveolar bone bending), and maxillary first molars (dental tipping). The stability of all three components after orthodontic treatment was also assessed by comparing changes between T0–T1 and T0–T2. Results: Post-expansion, angular measurements showed that skeletal expansion accounted for 87.50% and 88.56% of total expansion, alveolar bone bending for 7.09% and 5.23%, and dental tipping for 5.41% and 6.21% on the right and left sides, respectively. Post-treatment skeletal expansion relapsed by 11.20% and 13.28% on the right and left sides, respectively. Conclusions: The MSE mainly produces skeletal changes with insignificant and negligible dentoalveolar changes immediately after expansion. In the long term, the majority of skeletal expansion was maintained.



Citation: Ding, C.; Paredes, N.; Wu, B.; Moon, W. Long Term Skeletal, Alveolar, and Dental Expansion Effects of the Midfacial Skeletal Expander. *Appl. Sci.* **2023**, *13*, 9569. <https://doi.org/10.3390/app13179569>

Academic Editor: Jong-Moon Chae

Received: 30 July 2023

Revised: 15 August 2023

Accepted: 17 August 2023

Published: 24 August 2023



Copyright: © 2023 by the authors. Licensee MDPI, Basel, Switzerland. This article is an open access article distributed under the terms and conditions of the Creative Commons Attribution (CC BY) license (<https://creativecommons.org/licenses/by/4.0/>).

Keywords: expansion; alveolar bone bending; dental tipping; cone-beam computed tomography (CBCT); micro-implant-assisted rapid palatal expansion (MARPE)

1. Introduction

Maxillary transverse deficiency is one of the most common skeletal problems in the craniofacial region. However, it was demonstrated that the transverse dimension of the maxillary complex is the most malleable [1]. Traditionally, rapid palatal expansion (RPE) was the preferred standard treatment, especially for younger patients. Although the main purpose of RPE is to expand the maxilla by splitting the midpalatal suture, the surrounding circum-maxillary sutures are also affected [2]. In addition, dental tipping and alveolar bone bending are commonly observed [3–6]. RPE treatment for maxillary skeletal expansion is most effective when performed prior to the pubertal growth spurt, to minimize dentoalveolar side effects [7]. As patients mature and the midpalatal suture interdigitates, maxillary skeletal transverse expansion becomes more difficult, and the lateral forces from the tooth-borne RPE appliance are translated into more significant alveolar bone bending and dental tipping. This is true even in young patients, though to a lesser extent. These dentoalveolar changes can include fenestration, bone dehiscence, and a decrease in alveolar bone height [8].

In order to avoid these undesired dentoalveolar side effects, a variety of bone-supported or hybrid micro-implant-assisted rapid palatal expanders (MARPE) were introduced [9–19]. These MARPE appliances have grown in popularity in recent years as a potentially effective way to minimize dentoalveolar side effects in mature patients due to their ability to anchor directly onto bone. However, the results of different designs of MARPE appliances are varied, and significant dentoalveolar changes were still reported in many MARPE studies despite bone anchorage [11,14–20]. One study reported negligible molar tipping [21], while others claimed that side effects such as alveolar bone bending and dental tipping are not preventable but can be reduced compared to RPE [9,10].

The midfacial skeletal expander (MSE) is one particular design of MARPE appliance that has been described in the literature since 2014 [12,20–29]. There have been many studies on the use and successful application of the MSE in mature patients in recent years [12,21,28]. Cantarella et al. described a downward and outward movement of the zygomaticomaxillary complex in the coronal plane, with the fulcrum slightly localized above the frontozygomatic suture when performing expansion with the MSE [21]. However, the amount of skeletal, alveolar, and dental expansion achieved with RPE and MARPE were mostly measured using linear measurements rather than angular measurements and were based on arbitrary points [8–19,30].

Previous studies showed that MARPE expansions produce stable outcomes 1 year after expansion [31]. However, it was shown that MSE expansion is rotational in nature [21]. Two previous studies by Paredes et al. introduced a novel angular measurement system that takes into account the true fulcrum, providing a method to more accurately assess the rotational expansion created by the MSE [32,33]. These studies illustrated about 95% skeletal rotations and negligible dentoalveolar changes with the MSE immediately after expansion. Although the immediate result was groundbreaking, the stability of skeletal expansion can be questioned. The purpose of this study is to assess the long-term skeletal, alveolar, and dental expansion effects of the midfacial skeletal expander by comparing the changes immediately after expansion and at the completion of orthodontic treatment.

2. Materials and Methods

This retrospective study was performed at the University of California at Los Angeles (UCLA), with approval by the ethics committee (IRB number 17-000567). Pre-expansion CBCT images from 14 randomly selected patients successively treated with MSE (Biomaterials Korea, Seoul, Republic of Korea) with mean age of 20.4 ± 3.5 years were obtained. All patients were diagnosed with maxillary transverse deficit and treated at the orthodontic clinic, UCLA School of Dentistry, under the supervision of one clinician. Orthodontic treatment, including bonding of brackets and other appliances, was carried out after the completion of MSE expansion and acquisition of post-expansion CBCT. At the end of orthodontic treatment, the post-treatment CBCT was obtained. The selection criteria included (1) diagnosis of transverse maxillary deficiency; (2) patient records with CBCT images obtained at 3 time points: pre-expansion (T0), within 3 weeks after active expansion (T1), and at the end of orthodontic treatment (T2); (3) absence of any craniofacial irregularity; and (4) no orthodontic treatment precedent. The average time interval was 8.1 ± 4.8 months between pre-expansion and post-expansion CBCT and 19.5 ± 7.3 months between post-expansion and post-treatment. Average total treatment time between pre-expansion and post-treatment CBCT was 27.6 ± 6.9 months.

The transverse deficiency was diagnosed using coronal cuts from each subject's initial CBCT according to Paredes et al. [32]. The maxillary bone width was determined by the distance between the right and left bony points at the level of the mesiobuccal root tips of the upper first molars (usually the narrowest part of the maxilla). Mandibular bone width was defined as the distance between the right and left bony buccal surfaces at the level of the lower first molar furcation. If the mandibular width was greater than the maxillary width, a transverse discrepancy was diagnosed. Clinically and in dental casts, the maxillary width is defined by the distance between the left and right most concave points along the

maxillary vestibule above the mesiobuccal cusps of the first molars [34]. The mandibular width is defined as the distance between the left and right buccal surfaces over the lower first molar furcation. The amount of difference among these values also projects the extent of maxillary skeletal expansion required (Figure 1).

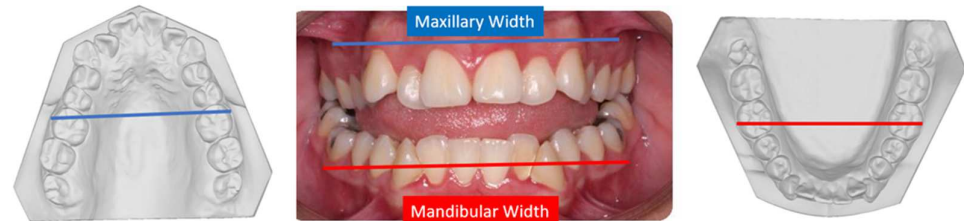


Figure 1. Method used clinically and in dental casts to project the extent of maxillary skeletal expansion required. Blue line (the distance between the narrowest points of the maxillary sulcus area above the mesiobuccal cusps of the first molars), maxillary width, and red line (the distance between the projected points on the mandibular buccal surfaces at the level of furcation), mandibular width, measured with a digital caliper.

Taking measurements on study models can be completed before and during the expansion in order to assess the bone relationship. The expansion was stopped once adequate expansion had been achieved, and the maxillary bony width became wider than the mandibular width for optimal occlusion after dental decompensation. The furcation is most likely the center of rotation for mandibular molars when compensated; therefore, the width between the buccal points over the furcation was used as the projected mandibular width after lower dental uprighting. The maxillary molars are generally buccally flared, and decompensation by uprighting the maxillary molars causes the maxillary dental arch to constrict. The most concave area of the maxilla is often at the apex of the maxillary molar, and controlled tipping with fulcrum at the apex is required for decompensation, unlike for mandibular molars.

The MSE II device (Figure 2) has a jackscrew unit (16.15 mm in length, 4.5 mm in width, and 14.15 mm in depth) with four parallel holes (1.8 mm in diameter) for micro-implant insertion and two soft supporting arms on each side, which are soldered to the molar bands for stabilizing MSE during the expansion. The body of MSE is positioned between the zygomatic buttress bones, usually located lateral to the first molars. Four micro-implants (1.8 mm in diameter and 11 mm or 13 mm in length) were bicortically inserted through the palatal bone. The posterior placement and bicortical engagements promote posterior and superior expansion of the maxillary process, which in turn produce the archial expansion described in previous studies [21,32,33]. The rate of expansion was 4–6 activations per day (0.133 mm per turn and ≈ 0.5 –0.8 mm per day) until a diastema appeared; then, the expansion rate changed to 1 activation per day. The activation was continued until the maxillary skeletal width was equal to or greater than the mandibular width. The MSE was kept in place, with no further activation for 6 months, to retain the expansion during bone formation.



Figure 2. Midfacial skeletal expander II device and head of activation key (MSE II, Biomaterials Korea, Seoul, Republic of Korea).

In addition to the pre-expansion CBCT, a second CBCT scan was obtained within 3 weeks of completing the expansion. The time interval between the scans was 8.1 ± 4.8 months, and this included the time that lapsed for administrative procedures, appliance fabrication, delivery, and treatment. In order to assess skeletal outcomes induced purely by MSE, post-expansion scans were obtained before patients received any other orthodontic appliances. All subjects must also have had a final post-treatment CBCT taken at the end of orthodontic treatment, with an average treatment time of 27.6 ± 6.9 months. The same scanner (5G; NewTom, Verona, Italy) was used for all patients, with an 18×16 cm field of view, 14-bit grayscale, and a standard voxel size of 0.3 mm. Configuration of the CBCT included scan time of 18 s (3.6 s emission time) with 110 kV. In order to properly adjust the milliamperes, an automated exposure control system was used to detect the patient's anatomic density. OnDemand3D (Version 2.0, Cybermed, Daejeon, Republic of Korea) software was used to superimpose all three CBCT images, using the anatomical structures of the entire anterior cranial base [35] by automated processing to match the voxel gray-scale patterns. Once the images were properly superimposed, equivalent slices were obtained without manual adjustments for further image analysis, with distance and angular measurements described below.

First, the pre- and post-expansion CBCT images (T0 and T1, respectively) were superimposed using the maxillary sagittal plane (MSP; passing through the anterior nasal spine, posterior nasal spine, and nasion), and the exact fulcrum location of each patient was identified utilizing the method described by Paredes et al. [32,33]. According to Paredes et al., the fulcrum was located near and slightly above the external surface of the frontozygomatic suture because sutures are the weakest points of the midfacial structure during the archial movement of expansion [21].

The true rotational fulcrum on the right and left sides (rF and lF) was found using a method previously described, and the interfrontal line was established by connecting rF and lF [32,33]. Then, the following angular measurements were performed to assess skeletal, alveolar, and dental components of expansion: (1) the frontozygomatic angle (FZA) between the interfrontal line and the line extending from fulcrum to the most external point of the zygomaticomaxillary suture, (2) the frontoalveolar angle (FAA) between the interfrontal line and the line extending from fulcrum to the alveolar bone surface at the level of distobuccal root tip of the upper first molars, and (3) the frontodental angle (FDA) between the interfrontal line and the line extending from fulcrum to the occlusal point located at the central groove of the upper first molar (Figure 3). These three angles were measured on right and left sides, and the pre-expansion value (T0) was subtracted from the post-expansion value (T1) in order to determine the treatment change for each section. The FZA changes correspond to zygomaticomaxillary expansion, a true skeletal expansion (FZA changes); the FAA changes correspond to the sum of skeletal expansion (FZA change) and alveolar bone bending (FAA changes–FZA changes); and the FDA changes correspond to the sum of skeletal expansion (FZA changes), alveolar bone bending (FAA changes–FZA changes), and dental tipping (FDA changes–FAA changes). In order to assess the long-term stability of MSE expansion, pre-expansion (T0) and post-treatment (T2) CBCTs were also superimposed using the method described, and all angular measurements described above were repeated to compare T0–T1 changes vs. T0–T2 changes.

Statistical Analysis

Based on the findings of a previous study [32], the minimum sample size for revealing significant changes after MSE and post-orthodontic treatment for this study was calculated as 14 patients. This was on the basis of a power of 0.85, an alpha of 0.05, and a mean difference of 1.0 ± 1.0 mm for lateral displacement of the zygomaticomaxillary complex.

Measurements were obtained for the 18 variables (6 pre-expansion, 6 post-expansion, and 6 post-treatment) on 5 randomly selected patients, by 2 raters, to assess method reliability. Measurements were then repeated after 2 weeks by the same operators. The calculated parameters were rater standard deviation, rater coefficient of variation, error

standard deviation, error coefficient of variation, and intra- and inter-class correlation coefficient (ICC).

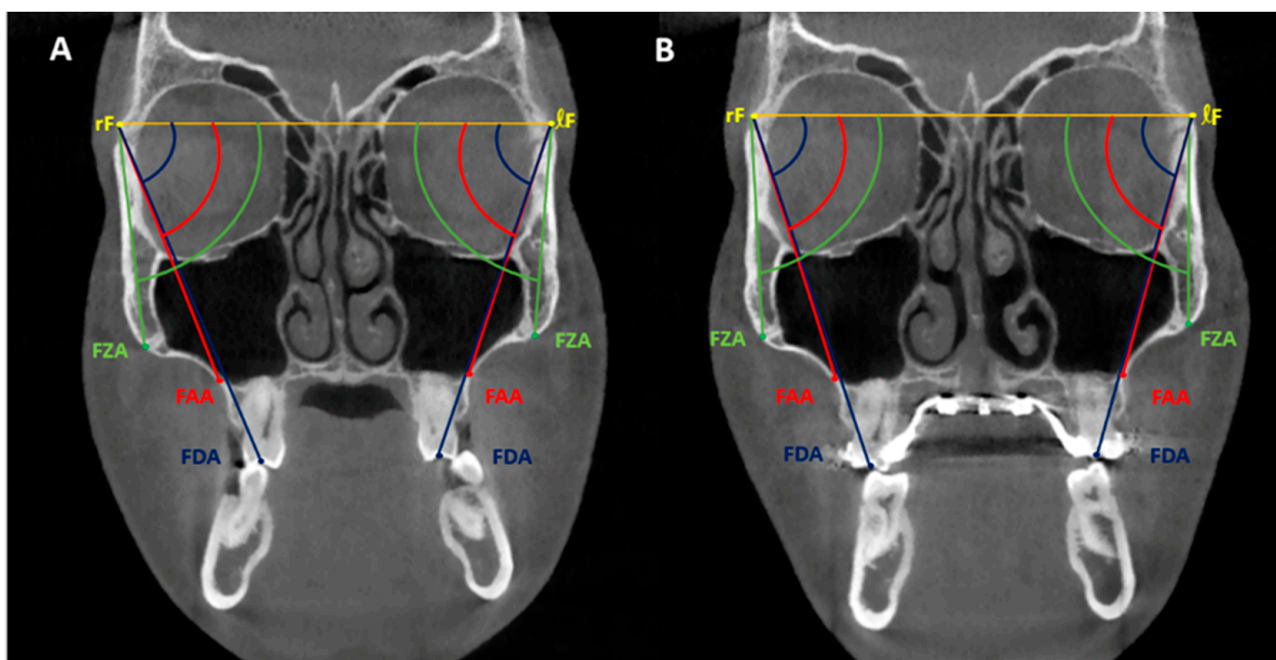


Figure 3. Angular measurement systems in the coronal zygomatic section: frontozygomatic angle (FZA); frontoalveolar angle (FAA); frontodental angle (FDA); rF, right fulcrum; lF, left fulcrum. Interfrontal line: yellow line connecting rF and lF. (A) Pre-expansion measurements. (B) Post-expansion measurements.

Shapiro–Wilk test was used to assess normality of the data distribution. Pre-expansion (T0), post-expansion (T1), and post-treatment (T2) variables were compared using a paired *t*-test for the normally distributed variables and Wilcoxon signed-rank test for the non-normally distributed variables. The significance level was set at $p < 0.05$. All data except for the FZA values at T0 were normally distributed, and Wilcoxon signed-rank test was applied only for the comparison with FZA at T0.

For each variable, the T0 values were subtracted from the T1 values. The percentages of skeletal expansion (a: the frontozygomatic angle changes), alveolar bone bending (b: the frontoalveolar angle change–the frontozygomatic angle change), and dental tipping (c: the frontodental angle change–the frontoalveolar angle change) were obtained. The value changes for each variable were compared to zero using a one-sample *t*-test ($p < 0.05$). Similarly, the T1 values were subtracted from the T2 values and compared to T0–T1 results to obtain the percentages of changes in skeletal expansion, alveolar bone bending, and dental tipping. Results were analyzed with a one-sample *t*-test compared to zero (control value), assuming that there would not be any changes without treatment since the subjects were non-growing patients ($p < 0.05$).

3. Results

For the considered parameters, the intra- and inter-class correlation coefficient (ICC) values were at 0.95 (95% confidence interval), showing that the measurements were highly reliable. The mean FZA, FAA, and FDA measurements at pre-expansion, post-expansion, and post-treatment are presented in Table 1.

A significant difference was found for the mean treatment change for all variables between T0 and T1 on both the right and left sides. Similarly, a significant difference was found for the mean treatment change for all variables between T0 and T2 as well as between T1 and T2 (Table 2).

Table 1. Skeletal, alveolar bone, and dental measurements.

	Variable	T0		T1		T2	
		Mean	SD	Mean	SD	Mean	SD
Right	FZA (°)	85.07	3.20	85.92	3.02	87.38	2.99
	FAA (°)	70.26	2.55	73.06	2.74	72.36	3.04
	FDA (°)	69.90	1.72	72.95	1.83	72.04	1.63
Left	FZA (°)	84.16	2.92	86.87	3.83	86.51	3.55
	FAA (°)	69.91	2.12	72.78	3.08	72.06	2.98
	FDA (°)	69.87	2.00	72.94	2.63	71.49	2.96

Table 2. Comparison of the skeletal, alveolar bone, and dental changes pre-expansion, post-expansion, and post-treatment using the paired *t*-test and Wilcoxon signed-rank test.

	Variable	T1-T0				T2-T0				T2-T1			
		Mean	SD	Z/t-Stat	<i>p</i> Value	Mean	SD	Z/t-Stat	<i>p</i> Value	Mean	SD	Z/t-Stat	<i>p</i> Value
Right	FZA (°)	2.59	1.30	Z = 3.18	0.001 *	2.31	1.36	Z = 3.18	0.001 *	-0.29	0.34	t = -3.15	0.008 *
	FAA (°)	2.80	1.08	t = 9.69	<0.001 *	2.11	1.42	t = 5.56	<0.001 *	-0.69	0.82	t = -3.17	0.007 *
	FDA (°)	2.96	1.23	t = 9.03	<0.001 *	2.05	1.08	t = 7.13	<0.001 *	-0.91	1.21	t = -2.80	0.015*
Left	FZA (°)	2.71	2.08	t = 4.88	<0.001 *	2.34	1.77	t = 4.95	<0.001 *	-0.36	0.46	t = -2.95	0.011 *
	FAA (°)	2.87	1.93	t = 5.58	<0.001 *	2.15	1.59	t = 5.05	<0.001 *	-0.72	0.67	t = -4.03	0.001 *
	FDA (°)	3.06	1.91	t = 6.01	<0.001 *	1.61	2.00	t = 3.02	0.01 *	-1.45	1.16	t = -4.69	<0.001 *

* *p* < 0.05.

Between T0 and T1, the total expansion consisted of 2.59 (±1.30) and 2.71 (±2.08) degrees of skeletal expansion, 0.21 (±0.51) and 0.16 (±0.67) degrees of alveolar bone bending, and 0.16 (±0.39) and 0.19 (±0.66) degrees of dental tipping on the right and left sides, respectively. These values represent 87.50% and 88.56% of skeletal expansion, 7.09% and 5.23% of alveolar bone bending, and 5.41% and 6.21% of dental tipping on the right and left sides, respectively (Table 3).

Table 3. Percentage of expansion at skeletal, alveolar bone, and dental components between pre- and post-expansion (T1-T0).

	Measurements	Skeletal Expansion			Alveolar Bone Bending		Dental Tipping
		Δa	Δb	Δc	Δa	Δb - Δa	Δc - Δb
Right	Mean (°)	2.59	2.80	2.96	2.59	0.21	0.16
	SD	1.30	1.08	1.23	1.30	0.51	0.39
				%	87.50%	7.09%	5.41%
				<i>p</i> value	<0.001 *	0.147	0.149
Left	Mean (°)	2.71	2.87	3.06	2.71	0.16	0.19
	SD	2.98	1.93	1.91	2.08	0.67	0.66
				%	88.56%	5.23%	6.21%
				<i>p</i> value	<0.001 *	0.388	0.301

* *p* < 0.05. Δa = change in FZA, Δb = change in FAA, and Δc = change in FDA.

Skeletal expansion was significant, while the alveolar bone bending and dental tipping values were not. Between T1 and T2, the total change consisted of -0.26 (±0.34) degrees and -0.36 (±0.46) degrees of skeletal change, -0.69 (±0.90) degrees and -2.51 (±1.92) degrees

of alveolar change, and $-0.91 (\pm 1.28)$ degrees and $-0.73 (\pm 1.02)$ degrees of dental change on the right and left sides, respectively. This suggests -11.20% and -13.28% of skeletal relapse compared to the amount of skeletal expansion gained from T0 to T1 on the right and left sides, respectively (Table 4). All changes in skeletal expansion, alveolar bone bending, and dental tipping were statistically significant.

Table 4. Percentage change in skeletal, alveolar bone, and dental components between post-expansion and post-treatment (T2–T1).

		T1–T0			T2–T1		
		Skeletal Expansion	Alveolar Bone Bending	Dental Tipping	Skeletal Expansion	Alveolar Bone Bending	Dental Tipping
		Δa	$\Delta b - \Delta a$	$\Delta c - \Delta b$	Δa	$\Delta b - \Delta a$	$\Delta c - \Delta b$
Right	Mean ($^{\circ}$)	2.59	0.21	0.16	-0.29	-0.69	-0.91
	SD	1.30	0.51	0.39	0.34	0.90	1.28
				%	-11.20%	-328.57%	-568.75%
				<i>p</i> value	<0.001 *	0.013 *	0.020 *
Left	Mean ($^{\circ}$)	2.71	0.16	0.19	-0.36	-2.51	-0.73
	SD	2.98	0.67	0.66	0.46	1.92	1.02
				%	-13.28%	-1568.75%	-384.21%
				<i>p</i> value	0.012 *	<0.001 *	0.019 *

* $p < 0.05$. Δa = change in FZA, Δb = change in FAA, and Δc = change in FDA.

4. Discussion

MARPE approaches are recommended to correct maxillary transverse discrepancies in adult patients, increasing the skeletal effect while minimizing the unwanted dentoalveolar side effects associated with traditional RPE expansion [9]. It was found that even in growing patients, RPE expansion produces the increased buccal flaring of the anchoring teeth regardless of the rate of activation [8] or the type of expander used [3,4,10,36–39]. Other adverse dentoalveolar effects include fenestration, dehiscence, and gingival recession [5], which are more common and critical in non-growing patients. In addition, expansion was found to relapse even in growing patients due to the relapse of dental tipping after the expansion phase [6,8]. The bone-borne nature of MARPE approaches is aimed at mitigating these adverse effects.

The MSE appliance is designed to achieve skeletal expansion by direct bony anchorage with four mini-implants placed next to the midpalatal suture and in between the zygomatic buttress bones with bicortical engagement [20]. The mini-implants allow force to be directly applied against the midpalatal suture with bands on the upper maxillary molars only for stability. The bicortical engagement of the mini-implant also allows the expansion to be more superiorly and posteriorly applied in the maxillary complex [20]. Paredes et al. [32] showed that the expansion achieved by the MSE appliance was significant and consisted of almost pure skeletal expansion with negligible and insignificant alveolar bone bending and slight dental tipping. Our results showed that skeletal expansion accounted for 87.50% (2.59 $^{\circ}$) on the right side and 88.56% (2.71 $^{\circ}$) on the left side. These values were comparable to those previously reported by Paredes et al. (96.58% R and 95.44% L) [32]. Furthermore, only the change in FZA was statistically significant, indicating that the observed expansion was mostly skeletal, with the midfacial structures rotating around the fulcrum points located near the frontozygomatic suture [21].

To date, studies on the long-term stability of MSE expansion are limited. A previous study on MARPE expansion found stable outcomes one year after expansion according to linear measurements [31], although the specific appliance used was different and did not have bicortical engagement. Furthermore, the results were linearly measured without taking into account the rotational nature of expansion. The T2 timepoint in our study reflects a mean

time of 19.5 ± 7.3 months post-expansion. According to our results, there was a significant skeletal rotational expansion of 2.31° on the right and 2.34° on the left from T0 to T2, with a statistically significant relapse of 11.20% (0.29°) and 13.28% (0.36°) on the right and left, respectively, between T1 and T2. However, this relatively minimal amount of relapse is a promising clinical result, especially compared to the amount of relapse noted using alternative methods such as surgically assisted rapid palatal expansion (SARPE). A long-term SARPE study by Chamberland and Proffit [40] illustrated that only 41% of total expansion was the skeletal component, and the rest of the expansion completely relapsed in 49 months. A meta-analysis by Schiffman and Tuncay looked at young Hyrax patients, and the long-term results indicated that the final width change was comparable to that of normal growth, suggesting a 100% relapse [41]. Byloff et al. [42] reported, in a longitudinal study of SARPE patients using a pre-fabricated Hyrax appliance, that the mean skeletal expansion of 1.3 mm had relapsed by 0.4 mm during the retention and post-retention periods, which represents a 30.77% relapse. Our findings suggest that MSE expansion may produce more stable results in non-growing patients, compared to both young Hyrax patients and mature SARPE patients. In the current study, an overexpansion based on bone width was not exercised, and expansion produced a slightly larger maxilla in order to produce a sound occlusal relationship; however, clinicians may consider the over-expansion of the MSE appliance by at least 10% in anticipation of some skeletal relapse in the long term.

The alveolar bone bending and dental tipping components varied greatly between T1 and T2, with alveolar bone measurements decreasing by 328.57% (0.69°) and 1568.75% (2.51°) and dental tipping measurements decreasing by 568.75% (0.91°) and 384.21% (0.73°) on the right and left, respectively. The significantly larger decrease in the alveolar and dental components post-treatment compared to the skeletal component can be attributed to the dental decompensation of the dentition during the orthodontic treatment after expansion. However, even after a relatively larger decrease in the FAA and FDA angles, the change in these angles from T0 to T2 is still significant (FAA = 2.11° R and 2.15° L; FDA = 2.05° R and 1.61° L), suggesting that true skeletal expansion was achieved and maintained.

Thus far, there have been limited data on the long-term stability of MSE expansion and MARPE in general. The MSE protocol used in our study involved keeping the MSE appliance passively installed for 6 months post-expansion for retention during bone formation, similar to the methods used in many previous studies [21,28,29,32,33]. However, perhaps a longer period of retention with mini-screws may improve expansion stability, allowing more time for bone formation.

Furthermore, due to MARPE being a relatively new technology, the current literature lacks any data regarding long-term stability beyond one year after MARPE expansion. Our study followed patients over a mean time period of around 19.5 months post-expansion. Although the results over the 19.5 months were promising, future studies are necessary to evaluate stability after 5 years or longer, for the accurate assessment of the long-term outcomes.

The limitation of the current study was the small sample size, due to the difficulties of acquiring a final CBCT, although the sample size was deemed to be adequate for statistical analysis. A robust study with a much larger sample size would be desirable. Another limitation was the lack of a true control group. The study group was compared to a 0 value, assuming that any changes without treatment would be a null value in non-growing patients. Further study with a prospective randomized control study would greatly improve the level of evidence.

5. Conclusions

1. MSE expansion mostly produced the skeletal rotational movement of midfacial structures with insignificant dentoalveolar changes immediately after expansion.
2. Skeletal expansion was significant both immediately post-expansion and post-orthodontic treatment.
3. The long-term losses of skeletal expansion were 11.20% (R) and 13.28% (L), and the majority of skeletal expansion was maintained.

4. The long-term dentoalveolar changes were in the magnitude of 300–1500% in the opposite direction, induced by the orthodontic decompensation of the pre-existing dental compensation; however, there were net gains in the intermolar width, despite these changes due to the long-term stability of skeletal expansion.

Author Contributions: C.D. and N.P.: design of the study, data collection, article writing, statistical analysis, interpretation of data, and evaluation of the statistical results. N.P. and W.M.: conceptualization and data interpretation. B.W.: study design, 3D evaluation, and visualization. B.W. and W.M.: supervision. All authors have read and agreed to the published version of the manuscript.

Funding: This research received no external funding.

Institutional Review Board Statement: The present study was approved by the ethics committee of the University of California, Los Angeles, IRB number 17-000567. All patients gave their written consent for their participation in the study.

Informed Consent Statement: Not applicable.

Data Availability Statement: The data of the current study are available from the corresponding author on request.

Conflicts of Interest: The authors declare no conflict of interest.

References

1. McNamara, J.A. Maxillary transverse deficiency. *Am. J. Orthod. Dentofac. Orthop.* **2000**, *117*, 567–570. [[CrossRef](#)]
2. Ghoneima, A.; Abdel-Fattah, E.; Hartsfield, J.; El-Bedwehi, A.; Kamel, A.; Kula, K. Effects of rapid maxillary expansion on the cranial and circummaxillary sutures. *Am. J. Orthod. Dentofac. Orthop.* **2011**, *140*, 510–519. [[CrossRef](#)] [[PubMed](#)]
3. Kılıç, N.; Kiki, A.; Oktay, H. A comparison of dentoalveolar inclination treated by two palatal expanders. *Eur. J. Orthod.* **2008**, *30*, 67–72. [[CrossRef](#)] [[PubMed](#)]
4. Ölmez, H.; Akin, E.; Karaçay, Ş. Multitomographic evaluation of the dental effects of two different rapid palatal expansion appliances. *Eur. J. Orthod.* **2007**, *29*, 379–385. [[CrossRef](#)] [[PubMed](#)]
5. Baysal, A.; Uysal, T.; Veli, I.; Ozer, T.; Karadede, I.; Hekimoglu, S. Evaluation of alveolar bone loss following rapid maxillary expansion using cone-beam computed tomography. *Korean J. Orthod.* **2013**, *43*, 83–95. [[CrossRef](#)]
6. Kartalian, A.; Gohl, E.; Adamian, M.; Enciso, R. Cone-beam computerized tomography evaluation of the maxillary dentoskeletal complex after rapid palatal expansion. *Am. J. Orthod. Dentofac. Orthop.* **2010**, *138*, 486–492. [[CrossRef](#)]
7. Baccetti, T.; Franchi, L.; Cameron, C.G.; McNamara, J.A. Treatment timing for rapid maxillary expansion. *Angle Orthod.* **2001**, *71*, 343–350. [[CrossRef](#)]
8. LaBlonde, B.; Vich, M.L.; Edwards, P.; Kula, K.; Ghoneima, A. Three dimensional evaluation of alveolar bone changes in response to different rapid palatal expansion activation rates. *Dent. Press J. Orthod.* **2017**, *22*, 89–97. [[CrossRef](#)]
9. Lin, L.; Ahn, H.W.; Kim, S.J.; Moon, S.C.; Kim, S.H.; Nelson, G. Tooth-borne vs bone-borne rapid maxillary expanders in late adolescence. *Angle Orthod.* **2015**, *85*, 253–262. [[CrossRef](#)]
10. Lagravère, M.O.; Carey, J.; Heo, G.; Toogood, R.W.; Major, P.W. Transverse, vertical, and anteroposterior changes from bone-anchored maxillary expansion vs traditional rapid maxillary expansion: A randomized clinical trial. *Am. J. Orthod. Dentofac. Orthop.* **2010**, *137*, 304e1-12, discussion 304-5.
11. Park, J.J.; Park, Y.-C.; Lee, K.-J.; Cha, J.-Y.; Tahk, J.H.; Choi, Y.J. Skeletal and dentoalveolar changes after miniscrew-assisted rapid palatal expansion in young adults: A cone-beam computed tomography study. *Korean J. Orthod.* **2017**, *47*, 77–86. [[CrossRef](#)] [[PubMed](#)]
12. Carlson, C.; Sung, J.; McComb, R.W.; Machado, A.W.; Moon, W. Microimplant-assisted rapid palatal expansion appliance to orthopedically correct transverse maxillary deficiency in an adult. *Am. J. Orthod. Dentofac. Orthop.* **2016**, *149*, 716–728. [[CrossRef](#)] [[PubMed](#)]
13. Lee, K.-J.; Park, Y.-C.; Park, J.-Y.; Hwang, W.-S. Miniscrew-assisted nonsurgical palatal expansion before orthognathic surgery for a patient with severe mandibular prognathism. *Am. J. Orthod. Dentofac. Orthop.* **2010**, *137*, 830–839. [[CrossRef](#)] [[PubMed](#)]
14. Mosleh, M.I.; Kaddah, M.A.; ElSayed, F.A.A.; ElSayed, H.S. Comparison of transverse changes during maxillary expansion with 4-point bone-borne and tooth-borne maxillary expanders. *Am. J. Orthod. Dentofac. Orthop.* **2015**, *148*, 599–607. [[CrossRef](#)]
15. Lombardo, L.; Carlucci, A.; Maino, B.G.; Colonna, A.; Paoletto, E.; Siciliani, G. Class III malocclusion and bilateral cross-bite in an adult patient treated with miniscrew-assisted rapid palatal expander and aligners. *Angle Orthod.* **2018**, *88*, 649–664. [[CrossRef](#)]
16. Seo, Y.-J.; Chung, K.-R.; Kim, S.-H.; Nelson, G. Camouflage treatment of skeletal Class III malocclusion with asymmetry using a bone-borne rapid maxillary expander. *Angle Orthod.* **2015**, *85*, 322–334. [[CrossRef](#)]
17. Vassar, J.W.; Karydis, A.; Trojan, T.; Fisher, J. Dentoskeletal effects of a temporary skeletal anchorage device-supported rapid maxillary expansion appliance (TSADRME): A pilot study. *Angle Orthod.* **2016**, *86*, 241–249. [[CrossRef](#)]

18. Wilmes, B.; Nienkemper, M.; Drescher, D. Application and effectiveness of a mini-implant- and tooth-borne rapid palatal expansion device: The hybrid hyrax. *World J. Orthod.* **2010**, *11*, 323–330.
19. Yılmaz, A.; Arman-Özçarpıcı, A.; Erken, S.; Polat-Özsoy, Ö. Comparison of short-term effects of mini-implant-supported maxillary expansion appliance with two conventional expansion protocols. *Eur. J. Orthod.* **2015**, *37*, 556–564. [[CrossRef](#)]
20. Lee, R.J.; Moon, W.; Hong, C. Effects of monocortical and bicortical mini-implant anchorage on bone-borne palatal expansion using finite element analysis. *Am. J. Orthod. Dentofac. Orthop.* **2017**, *151*, 887–897. [[CrossRef](#)]
21. Cantarella, D.; Dominguez-Mompell, R.; Moschik, C.; Mallya, S.M.; Pan, H.C.; Alkahtani, M.R.; Elkenawy, I.; Moon, W. Midfacial changes in the coronal plane induced by microimplant-supported skeletal expander, studied with cone-beam computed tomography images. *Am. J. Orthod. Dentofac. Orthop.* **2018**, *154*, 337–345. [[CrossRef](#)]
22. MacGinnis, M.; Chu, H.; Youssef, G.; Wu, K.W.; Machado, A.W.; Moon, W. The effects of micro-implant assisted rapid palatal expansion (MARPE) on the nasomaxillary complex—A finite element method (FEM) analysis. *Prog. Orthod.* **2014**, *15*, 52. [[CrossRef](#)] [[PubMed](#)]
23. Brunetto, D.P.; Sant’anna, E.F.; Machado, A.W.; Moon, W. Non-surgical treatment of transverse deficiency in adults using Microimplant-assisted Rapid Palatal Expansion (MARPE). *Dent. Press J. Orthod.* **2017**, *22*, 110–125. [[CrossRef](#)]
24. Suzuki, S.S.; Braga, L.F.S.; Fujii, D.N.; Moon, W.; Suzuki, H. Corticopuncture Facilitated Microimplant-Assisted Rapid Palatal Expansion. *Case Rep. Dent.* **2018**, *2018*, 1392895. [[CrossRef](#)]
25. Abedini, S.; Elkenawy, I.; Kim, E.; Moon, W. Three-dimensional soft tissue analysis of the face following micro-implant-supported maxillary skeletal expansion. *Prog. Orthod.* **2018**, *19*, 46. [[CrossRef](#)] [[PubMed](#)]
26. Garcez, A.S.; Suzuki, S.S.; Storto, C.J.; Cusmanich, K.G.; Elkenawy, I.; Moon, W. Effects of maxillary skeletal expansion on respiratory function and sport performance in a para-athlete—A case report. *Phys. Ther. Sport* **2019**, *36*, 70–77. [[CrossRef](#)]
27. Storto, C.J.; Garcez, A.S.; Suzuki, H.; Cusmanich, K.G.; Elkenawy, I.; Moon, W.; Suzuki, S.S. Assessment of respiratory muscle strength and airflow before and after microimplant-assisted rapid palatal expansion. *Angle Orthod.* **2019**, *89*, 713–720. [[CrossRef](#)]
28. Cantarella, D.; Dominguez-Mompell, R.; Mallya, S.M.; Moschik, C.; Pan, H.C.; Miller, J.; Moon, W. Changes in the midpalatal and pterygopalatine sutures induced by micro-implant-supported skeletal expander, analyzed with a novel 3D method based on CBCT imaging. *Prog. Orthod.* **2017**, *18*, 34. [[CrossRef](#)]
29. Cantarella, D.; Dominguez-Mompell, R.; Moschik, C.; Sfogliano, L.; Elkenawy, I.; Pan, H.C.; Mallya, S.M.; Moon, W. Zygomatico-maxillary modifications in the horizontal plane induced by micro-implant-supported skeletal expander, analyzed with CBCT images. *Prog. Orthod.* **2018**, *19*, 41. [[CrossRef](#)] [[PubMed](#)]
30. Luebbert, J.; Ghoneima, A.; Lagravère, M.O. Skeletal and dental effects of rapid maxillary expansion assessed through three-dimensional imaging: A multicenter study. *Int. Orthod.* **2016**, *14*, 15–31. [[CrossRef](#)]
31. Lim, H.-M.; Park, Y.-C.; Lee, K.-J.; Kim, K.-H.; Choi, Y.J. Stability of dental, alveolar, and skeletal changes after miniscrew-assisted rapid palatal expansion. *Korean J. Orthod.* **2017**, *47*, 313–322. [[CrossRef](#)]
32. Paredes, N.; Colak, O.; Sfogliano, L.; Elkenawy, I.; Fijany, L.; Fraser, A.; Zhang, B.; Moon, W. Differential assessment of skeletal, alveolar, and dental components induced by microimplant-supported midfacial skeletal expander (MSE), utilizing novel angular measurements from the fulcrum. *Prog. Orthod.* **2020**, *21*, 18. [[CrossRef](#)]
33. Paredes, N.A.; Colak, O.; Sfogliano, L.; Elkenawy, I.; Fijany, L.; Torres, M. Defining Fulcrums for Craniofacial Structures with Midfacial Skeletal Expander (MSE) Treatment and Applying Novel Angular Measurement System for Accurate Assessments. *Clin. Case Rep. Int.* **2022**, *6*, 1448.
34. Andrews, L.F.; Andrews, W. The six elements of orofacial harmony. *Andrews J. Orthod. Orofac Harmon.* **2000**, *1*, 13–22.
35. Cevidanes, L.; Bailey, L.; Tucker, G.; Styner, M.; Mol, A.; Phillips, C.; Proffit, W.; Turvey, T. Superimposition of 3D cone-beam CT models of orthognathic surgery patients. *Dentomaxillofacial Radiol.* **2005**, *34*, 369–375. [[CrossRef](#)] [[PubMed](#)]
36. Christie, K.F.; Boucher, N.; Chung, C.-H. Effects of bonded rapid palatal expansion on the transverse dimensions of the maxilla: A cone-beam computed tomography study. *Am. J. Orthod. Dentofac. Orthop.* **2010**, *137*, S79–S85. [[CrossRef](#)]
37. Weissheimer, A.; de Menezes, L.M.; Mezomo, M.; Dias, D.M.; de Lima, E.M.S.; Rizzato, S.M.D. Immediate effects of rapid maxillary expansion with Haas-type and hyrax-type expanders: A randomized clinical trial. *Am. J. Orthod. Dentofac. Orthop.* **2011**, *140*, 366–376. [[CrossRef](#)]
38. Ciambotti, C.; Ngan, P.; Durkee, M.; Kohli, K.; Kim, H. A comparison of dental and dentoalveolar changes between rapid palatal expansion and nickel-titanium palatal expansion appliances. *Am. J. Orthod. Dentofac. Orthop.* **2001**, *119*, 11–20. [[CrossRef](#)]
39. Asanza, S.; Cisneros, G.J.; Nieberg, L.G. Comparison of Hyrax and bonded expansion appliances. *Angle Orthod.* **1997**, *67*, 15–22. [[CrossRef](#)]
40. Chamberland, S.; Proffit, W.R. Short-term and long-term stability of surgically assisted rapid palatal expansion revisited. *Am. J. Orthod. Dentofac. Orthop.* **2011**, *139*, 815–822. [[CrossRef](#)]
41. Schiffman, P.H.; Tuncay, O.C. Maxillary expansion: A meta analysis. *Clin. Orthod. Res.* **2001**, *4*, 86–96. [[CrossRef](#)] [[PubMed](#)]
42. Byloff, F.K.; Mossaz, C.F. Skeletal and dental changes following surgically assisted rapid palatal expansion. *Eur. J. Orthod.* **2004**, *26*, 403–409. [[CrossRef](#)] [[PubMed](#)]

Disclaimer/Publisher’s Note: The statements, opinions and data contained in all publications are solely those of the individual author(s) and contributor(s) and not of MDPI and/or the editor(s). MDPI and/or the editor(s) disclaim responsibility for any injury to people or property resulting from any ideas, methods, instructions or products referred to in the content.